GAMMA DOSE CALCULATIONS IN THE TARGET SERVICE CELL OF THE SNS

Y. Y. Azmy, J. O. Johnson, R. A. Lillie, R. T. Santoro
Oak Ridge National Laboratory
P. O. Box 2008
Oak Ridge, TN 37831
(423) 574-8069

ABSTRACT

Calculations of the gamma dose rates inside and outside of the Target Service Cell (TSC) of the Spallation Neutron Source (SNS) are complicated by the large size of the structure, large volume of air (internal void), optical thickness of the enclosing walls, and multiplicity of radiation sources. Furthermore, a reasonably detailed distribution of the dose rate over the volume of the TSC, and on the outside of its walls is necessary in order to optimize electronic instrument locations, and plan access control. For all these reasons a deterministic transport method was preferred over Monte Carlo. The three-dimensional neutral particle transport code TORT was employed for this purpose with support from other peripheral codes in the Discrete Ordinates of Oak Ridge System (DOORS). The computational model for the TSC is described and the features of TORT and its companion codes that enable such a difficult calculation are discussed. Most prominent is the presence of severe ray effects in the air cavity of the TSC that persists in the transport through the concrete walls and is pronounced throughout the problem volume. Initial attempts at eliminating ray effects from the computed results using the newly developed three-dimensional uncollided flux and first collided source code GRTUNCL3D are described.

I. INTRODUCTION

The Target Service Cell (TSC) of the Spallation Neutron Source (SNS) is a large room 31m × 12m × 6m in size, constructed from heavy concrete and lined on the inside with 0.0048m thick stainless steel. For the most part, the inside of the TSC is air, or void as far as the photon transport process is concerned, punctuated with many details such as internal walls and structures, leaded glass windows, etc. Several fixed sources of photons are located inside of the TSC including the shroud cooling water, circulating mercury pipes and pump, and several target components at various stages of processing. Given the early stage in the design of the SNS, it is expected that the model of the TSC will evolve as the design matures. So the reader is warned that the model and results presented in this paper are in a state of flux and are not representative of the final design of the TSC. Details of the TSC configuration used to construct the TORT model employed in the calculations presented in this paper are depicted in Fig. 1.

The desire to obtain the flux and dose rate distributions inside of the TSC as well as on the outside walls makes a deterministic transport calculation the only viable option. This choice is reinforced by the large physical dimensions of the TSC, the optical thickness of the concrete walls (amounting to deep penetration transport to compute the outside dose), and the multiple sources of radiation. Obtaining good statistics on the detailed information required from this calculation with a Monte Carlo model we conjecture is prohibitively expensive with respect to project timelines. Nevertheless, deterministic methods present a few challenges that must be overcome in order to obtain a reliable and robust computational procedure. These challenges include: Accuracy (mesh size, order of the angular quadrature, order of the Legendre representation of scattering angular anisotropy, iterative convergence, ray effects, etc.); computational efficiency (execution time, memory requirement, and disk space); post-processing of the results (visualization, editing, etc.).

In this paper we present initial attempts at meeting these challenges. We describe the steps involved in constructing the computational model of the TSC for the state of the art, three-dimensional, discrete ordinates neutral particle transport code TORT.[1] In Sec. II we summarize preliminary computations that feed into the TORT model. In Sec. III we include results of computations conducted to date. We conclude the paper with our plans for improving on the TORT computational model in the next round of calculations for the TSC with the latest design configuration in Sec. IV.

II. TORT COMPUTATIONAL MODEL

Neutral particle transport problems in the applied world tend to be very difficult. The dimensionality of the phase space, six in the case of steady state three-dimensional problems, and the level of detail and accuracy required of the solution result in large discrete-variable arrays that must

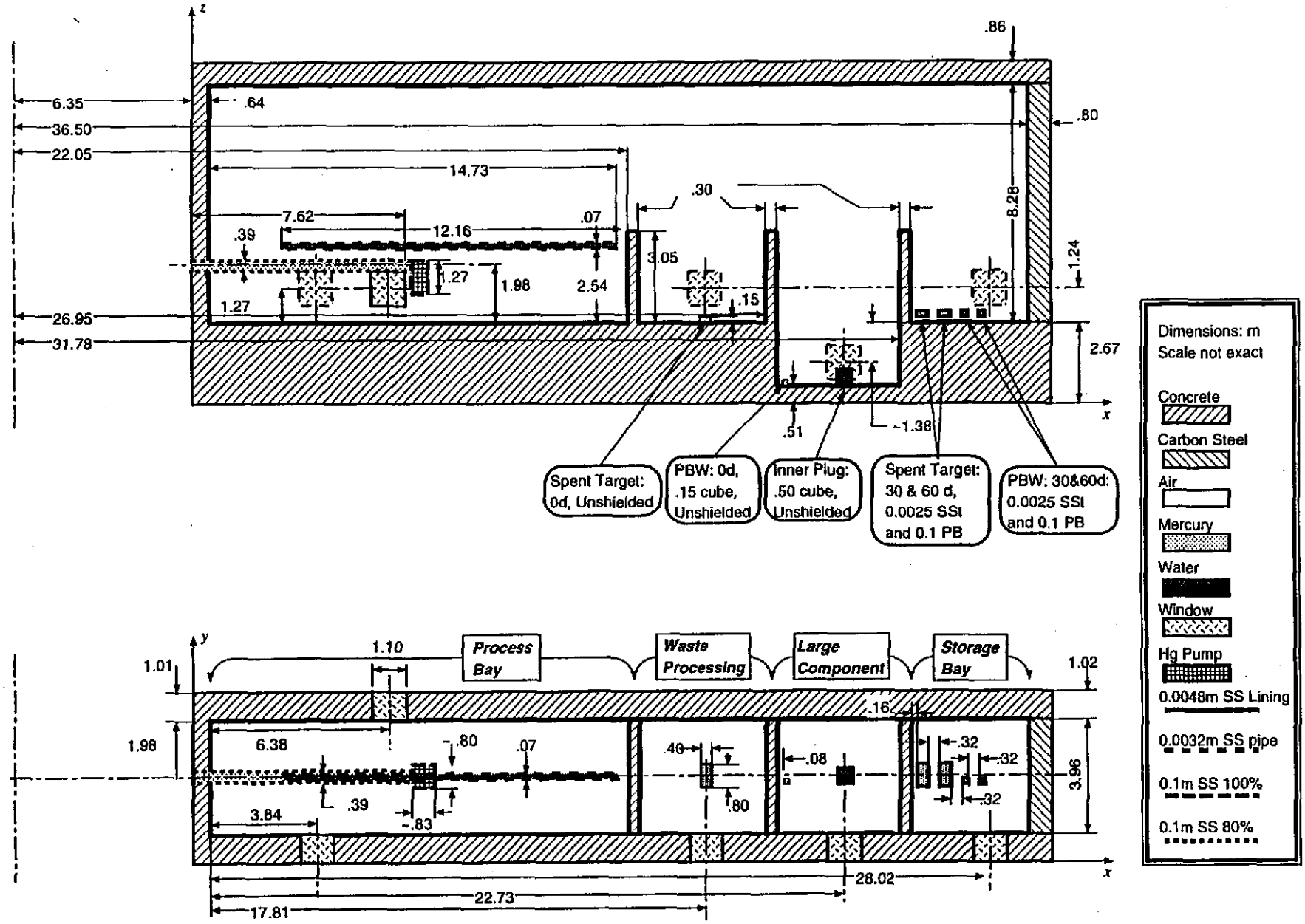

Fig. 1. TORT Model of the Target Service Cell Configuration

be computed and stored thus straining computational resources. In addition, the nature of the solution to such problems is typically fraught with discontinuities, sharp gradients, and other features that burden most any general purpose numerical method or algorithm. The TORT code was designed to deal with such difficulties by providing the user with a large collection of options and adjustable parameters that address a wide variety of such difficulties.[1] Default settings and parameter values are provided for the novice user and as a starting point for the advanced user. If inadequacies in the results are identified the user can then adjust the settings to improve the solution or code performance in subsequent runs. In addition, peripheral codes accompanying TORT in the Discrete Ordinates of Oak Ridge System (DOORS) package supplement this capability by affording the user means to break up the problem into pieces that can be solved in stages feeding into one another.[2] In this section we outline our strategy to construct a TORT model for the TSC and execute the code successfully on a single node of the IBM SP2 computer via LoadLeveler.

A. Geometry

As evident from Fig. 1 the geometric configuration of the TSC naturally lends itself to Cartesian geometry where the fine detail of pipe curvature and so on can be easily and accurately approximated. While TORT sets no limitations on the shape and size of computational cells it is prudent to observe some elementary rules in constructing the mesh. First, it is important to design the Cartesian grid so that most cells are as close to cubic in shape as possible. The streaming part of the discretized transport operator tends to become inaccurate in cells with odd aspect ratios. Similarly, the discontinuous mesh feature in TORT allows the user great flexibility in designing the computational mesh but at a cost to local accuracy of the solution. Hence, in our judgement odd-shaped cells and discontinuous mesh must be avoided if possible; if necessary they should be confined to regions in the problem domain where the accuracy of the results is not of great importance. Since the dose rate distribution is desired almost everywhere inside of the TSC and outside its walls the only regions where local accuracy is not crucial are in the immediate neighborhood of the sources and inside of the concrete walls. These are relatively small compared to the total volume of the TSC hence we apply these requirements on the mesh everywhere.

Next, we compute the average size of a cell in the model. Clearly the total memory requirement of TORT as well as execution time are proportional to the number of computational cells in the model, among other parameters. Hence, the available computational resources can be roughly translated into a maximum number of computational cells, N. From the dimensions of the TSC shown in Fig. 1 the average *cubic* cell size is the cubic root of 30.95m × 5.99m × 11.81m / N. For N = half, and one million cells, the average cell size must be about 0.16m, and 0.13m, respectively. The approximate number of cells in the x, y, and z dimension in the 500,000 cell case, for example, is 194, 38, and 74, respectively.

Using these figures as guidelines, we go through the details of the TSC configuration determining cell boundaries and smearing structures that are much smaller than 0.16m over the volume of a cell preserving the material and source density. For example the stainless steel lining of the TSC interior would have resulted in cells with aspect ratio in excess of 30 had it been modeled in its nominal thickness of 0.0048m. Instead, we smeared it over a layer of cells .08m thick reducing the aspect ratio of the resulting cells to about 2. After the interior detail was modeled, the resulting grid comprised 206 × 43 × 80 = 708,640 cells.

B. Cross Sections

The cross section data for this problem were mixed from the DABL69[3] library, a multigroup cross-section library generated from ENDF/B-V data for use in defense-related radiation shielding applications. The library is available in a broad-group (46-neutron, 23-photon) energy structure and P_5 anisotropic scattering representation. The establishment of specifications for the library, especially the specific group structure and energy weighting functions, was an important part of the generation of the library. The energy group structure contains some special tailoring to the oxygen and nitrogen cross sections and improved energy resolution in the range of 100-1000 keV where the iron cross section is highly structured. The library contains most materials of importance in defense-related shielding problems and includes several reference source spectra and response functions. DABL69 is available in two formats including the commonly used ANISN format and the more versatile AMPX master format.

Since we are not concerned with neutron transport in the present calculation, and since the gamma sources do not exceed 8 MeV we extract the binary data for the last 19 groups from the DABL69 library. This is used in the cross-section manipulation code GIP[4] to mix macroscopic cross sections for the materials in the TSC. For simplicity, air inside the room is approximated by zero-density hydrogen, and nuclides appearing in material mixtures but unavailable in the DABL69 library are approximated by the closest lower Z available material in order to ensure conservatism of the results. Flux to dose conversion factors

for the ensuing 19 group calculation are obtained from the DABL69 library data.

C. Distributed Sources

To address the shielding requirements of the TSC for the distributed activation sources, we adopted the following procedure. The target station was modeled (by component) in the HETC[5]and MCNP[6] codes to provide the required input data for the isotope generation and depletion code, ORIHET95[7]. ORIHET95 utilizes a matrix-exponential method to study the buildup and decay of activity for any system for which the nuclide production rates are known. The combination of the HETC- and MCNP-generated sources yielded the radionuclide concentrations, radioactivity, and time dependent decay gamma source spectra, as a function of generation (buildup) time and depletion (decay), for input into the DOORS discrete ordinates deterministic transport codes.

The activation of the Hg target, coolant water, and target components during operation and as a function of time after accelerator shutdown was presented previously.[8] Activation data were obtained for reactions of 1-GeV protons (at 1 mA) incident on these components. Tabular data generated as described in Ref. 8 were formatted to facilitate their use in TORT.

D. Preliminary Tests

In large applications like the one at hand where a calculation will be performed, perhaps with some modifications, repeatedly it is worthwhile to experiment with some execution parameters and determine their effect on the solution and computational performance from the outset. These tests were conducted using an earlier model of the TSC, a one-group cross-section set collapsed from DABL69 using the spectrum in concrete, and a fictitious one-group source overlapping the mercury pipe. In spite of these differences we conjecture that the conclusions reached should apply to the TSC full model calculation. In all cases described here, and in the full model calculations we employed an S_6 fully symmetric angular quadrature set, and a 10^{-3} pointwise relative convergence criterion on the scalar flux.

In the testing stage we focused on four factors:
1. Solution method: Theta-Weighted *vs* Linear Nodal;
2. Cell size: 644,640 *vs* 4,462,200 cell model;
3. Acceleration mesh: 1932-cell *vs* fine-mesh acceleration;
4. Scattering anisotropy representation: P_1 *vs* P_3.

The main conclusion is that, as anticipated, the Linear Nodal, fine mesh model, and P_3 runs consume longer times to complete than runs with each of their alternative options. Employing a coarse mesh for acceleration did not seem to reduce turn-around time significantly, and in fact slightly impeded convergence measured in number of iterations. Hence, specification of a coarse mesh for the Partial Current Rebalance calculation in the production runs was abandoned, and by default TORT employs the same mesh on which the mesh sweeps are performed to conduct the acceleration stage. All options listed above exhibited poor convergence at locations where the flux is extremely small. TORT provides the capability of bypassing the convergence test for the scalar flux if it falls below a user-specified threshold. Since the permissible dose outside the TSC is of the order of a fraction of a mrem/hr, and in view of the magnitude of the flux to dose convergence factors this cutoff was set to 10^{-3} in the production runs.

The most serious problem with the solution identified by these test runs is the severe, and undesirable, ray effects observed in the air surrounding the mercury pipe, effects that persisted even after transport through the concrete walls. Ray effects are a consequence of the discrete ordinates approximation of the angular dependence in the transport equation and typically characterize the transport of neutral particles in air and weakly scattering materials. Solutions exhibiting ray effects usually overestimate the flux along discrete ordinate rays emanating from localized sources and underestimate it over large regions of the model. The easiest way to overcome this difficulty is to raise the order of the angular quadrature. However, in this problem this could result in a significant increase in computation time; and due to the large disparity between the physical sizes of the TSC and the individual sources, will require an unrealistically high order set to sufficiently eliminate ray effects. Another way to deal with such effects is to generate a distributed first collision source with the GRTUNCL3D code,[9] use it to drive a TORT calculation, then sum the contribution to the dose from the uncollided and fully-collided calculations as a postprocess. GRTUNCL3D is designed to execute off of a TORT input file with a few additional control parameters and source data provided in a separate input file, thus reducing the burden on the user and the potential for input error to a minimum.

III. COMPUTATIONAL RESULTS

Comparing the general features of the dose rate distribution on the inside and outside walls of the TSC obtained in the testing stage exhibited good agreement, especially in view of the strong ray effects. There is no question that the dose rate inside the TSC must be computed with GRTUNCL3D, but the potential for reduced ray effects in the production calculation on the outside walls is justified on two accounts. First, the multiple sources in the production configuration could cause many more regions in the TSC to be directly illuminated by at

least one source that dominates the dose over that region. Second, the transport of the radiation through the thick concrete walls should sharply attenuate the uncollided flux, which is affected the most by ray effects, and redirect the paths of photons towards points that are not directly illuminated by any source. In essence the conjecture is that transport through a few mean free paths (mfp) of concrete would have reduced the uncollided photon flux to the point that the scattering source dominates the group scalar flux, hence the dose. This is more likely in the multigroup calculation because the photons have an additional opportunity to scatter across angles while slowing down.

Hence, we proceeded with the TORT computation for the TSC configuration with 19 energy groups, and distributed sources in the mercury pipe and pump, water pipe, and target components. For the Theta-Weighted (TW) and Linear Nodal (LN) methods all but a few groups converged; for the groups that did not converge fully, the maximum relative change in the scalar flux was smaller than .01. These runs are very long, ~20 hr. for TW and ~35 hr. for LN, and result in large flux files, 0.9 and 1.1 GB, respectively. Contour maps of the dose rate inside and outside the TSC were generated using the XTORID and ISOPLOT codes from ORNL's DOORS package.[10] The solutions with the two methods agreed pretty well in general, thus raising our confidence level in the obtained solution.

Contour maps of the dose rate in the *y-z* plane at the center of the first air cell inside of the left wall, and in the *x-z* plane at the center of the first concrete cell of the near wall (with the four windows), are illustrated in Figs. 2.a, and 2.b, respectively. As discussed above, the ray effects displayed in the air in Fig. 2.a with their typical finger-shaped design are not surprising. Their existence in Fig. 2.b, outside of the concrete walls, in the form of high intensity horizontal lines parallel to the mercury pipe, and high intensity islands in the right half of the TSC where the target components are located is a disappointment. The failure of our conjecture was investigated in search of an explanation.

First, we checked the group contributions to the dose on the roof of the TSC, as an example, to see if it was dominated by the first group. Had this been the case, the top group does not have scattering into it from other groups thus diminishing the potential for smoothing out the ray effects by the scattering operator. As it turns out the second group accounts for more than 25% of the maximum dose on the roof, large but not sufficient to explain the ray effects outside given that most other groups contributed almost equally to the dose rate.

Next, to examine the influence of forward peaking of the scattering on the solution we performed a P_0 (isotropic) scattering order calculation with TW. [Note that TORT permits the transport calculation to use a different expansion order for the scattering anisotropy than specified in the cross section set, hence a minor modification to the input file was necessary to execute the P_0 calculation]. Since the resulting solution suffered essentially the same ray effects as the P_3 solution we conclude that forward peaking is not the sole, or main, reason for the ray effects on the external walls of the TSC.

Finally, to test the possibility that large removal cross sections, at least in the dose-dominating energy groups, were the main cause for the sharp exterior ray effects, we constructed a cross-section set in which all scattering cross sections were set to zero. Had the resulting dose on the TSC exterior compared closely to the fully collided dose we would have concluded that dominance of the removal process over the total interaction rate is responsible for the severe ray effects. This was not the case though, and we are led to conclude that a combination of the above reasons causes the observed ray effects, with no one reason dominating the others. It is evident at this point that computing the uncollided flux and first collided source via GRTUNCL3D is necessary for determining the dose rate both inside and outside the TSC.

As discussed earlier minor additional input, beyond the TORT input file, is necessary to execute GRTUNCL3D. Two approximations were necessary to facilitate this run:

1. The distributed sources used in TORT had to be concentrated at discrete points as required by GRTUNCL3D.[9] This is reasonable because the physical dimensions of the distributed sources are very small in comparison with the full dimensions of the TSC. [In fact this is partly responsible for the ray effects that necessitated the GRTUNCL3D run]. Hence we collapsed each of the targets, target noses, Proton Beam Windows (PBW), and mercury pump sources to a point source located at the respective center of mass and scaled the point source strength to account for the original distributed source volume. The distributed sources in the mercury, and water pipes were collapsed to 48, and 76 equally spaced point sources, respectively, along the respective pipe axes, and we scaled their strengths to conserve the total strength of the distributed sources.
2. Self-shielding effects of the materials of all the collapsed sources could result in smaller fluxes outside of these materials than if the sources were truly distributed. In order to bias the approximation towards producing a conservative, overestimate of the flux, hence the dose also, we set to zero the density of the materials of the distributed sources in the

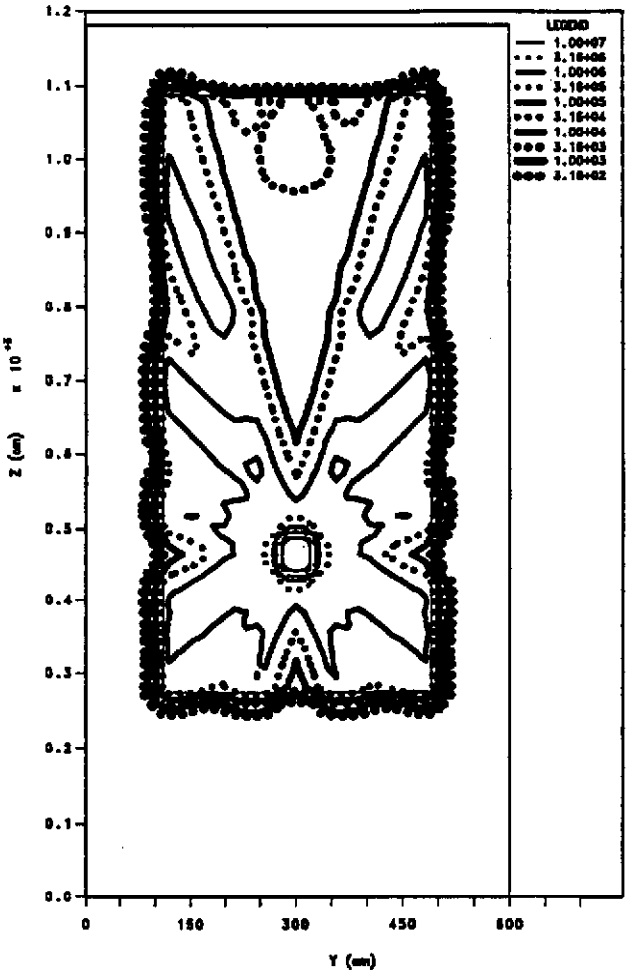

Fig. 2.a. Dose Contour Map (mrem/h) with TW Method Over y-z Plane in First Air Cell Inside the Left Wall Without GRTUNCL3D Source

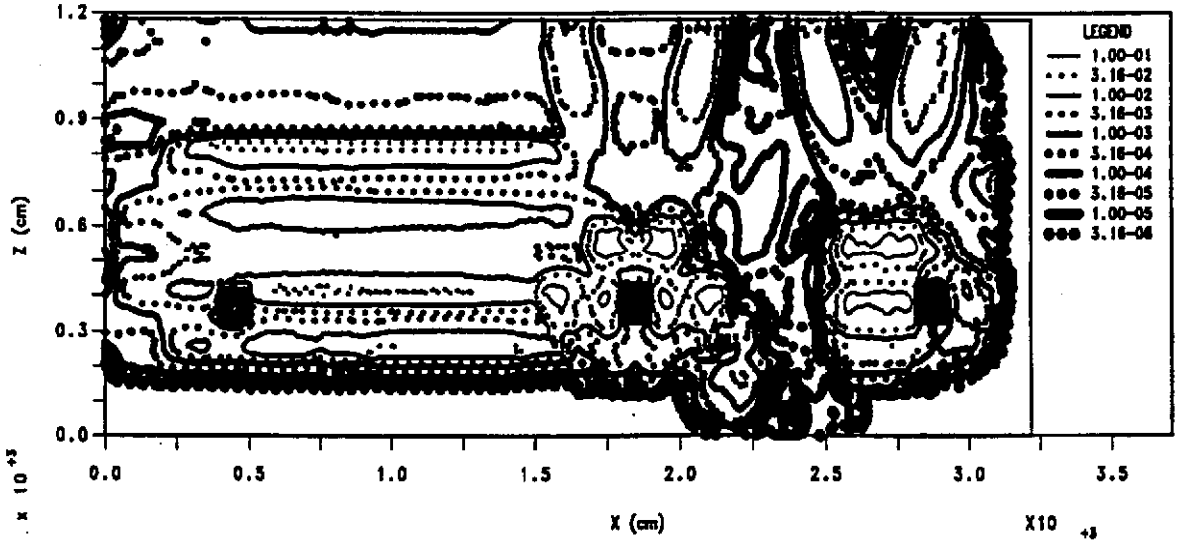

Fig. 2.b Dose Contour Map (mrem/h) with TW Method Over y-z Plane in First Concrete Cell of Near Wall Without GRTUNCL3D Source

AZMY

GRTUNCL3D run. The original densities were restored in the subsequent TORT run that employed the GRTUNCL3D-computed first-collision source to compute the collided flux over the entire TSC.

Due to the large number of sources and cells, execution of GRTUNCL3D takes several days to complete. Following this, TORT is executed then the uncollided flux from GRTUNCL3D and the collided flux from TORT for each group and computational cell are added and then folded with the flux-to-dose conversion factors. Contour maps of the resulting dose-rate distribution are generated as described above. The contour map for the dose at the same x position as in Fig. 2.a is depicted in Fig. 3. Clearly, there are still ray effects in this figure, but they are less severe than in Fig. 2.a. The persistence of the ray effects even when using the first-collided source is due to collisions in the mercury pipe and shield which again transport through air along discrete ordinates as before. The same behavior is observed for the other sources in this configuration as illustrated in Fig. 4 for the x-z planes at the centers of the first concrete cell of the near wall, and of the first air cell immediately inside of it, and in Fig. 5 for the x-y planes at the centers of the last air cell below the ceiling, and of the last concrete cell on the roof.

IV. CONCLUSION

We constructed a TORT model of the SNS TSC and conducted gamma dose calculations using 19 energy groups and an S_6 fully symmetric angular quadrature. The difficulty of this calculation arises from the sheer size of the problem on the one hand, and the level of detail and accuracy required for the proper and economic design of the TSC on the other. Various TORT parameter settings were tested to identify the best and most efficient computational approach for this problem. Aside from long computational times and large memory requirements, the greatest difficulty encountered is the occurrence of ray effects. Our first attempt to eliminate these by separately computing the uncollided and fully collided flux only reduced their severity. One-dimensional calculations modeling the mercury pipe, shield, air, and concrete walls in cylindrical geometry produced dose rates on the inside and the outside of the concrete wall that are within the range defined by the high and low magnitudes of the ray effects-infected dose computed with TORT. Furthermore, we have identified an improved computational procedure that we believe will completely eliminate ray effects from the TORT solution. We will adjust the strengths of the point sources in GRTUNCL3D to account for the containment wall and shielding thereby eliminating the need for modeling these materials in computing the first collided source. As a result the photons should experience their first collisions in the stainless steel lining after traversing the air cavity thus eliminating primary ray effects entirely. This computation is currently underway.

REFERENCES

1. W. A. Rhoades and D. B. Simpson, "The TORT Three-Dimensional Discrete-Ordinates Neutron/Photon Transport Code, ORNL/TM-13221 (1997).

2. Y. Y. Azmy, "The Three-Dimensional, Discrete Ordinates Neutral Particle Transport Code TORT: An Overview," *OECD/NEA Meeting on 3D Deterministic Radiation Transport Computer Programs, Features, Applications, and Perspectives*, Dec. 2-3, 1996, Paris, France, p. 197, OECD, Paris, France (1996).

3. D. T. Ingersoll, R. W. Roussin, C. Y. Fu, and J. E. White, "DABL69: A Broad-Group Neutron/Photon Cross-Section Library for Defense Nuclear Applications," ORNL/TM-10568, Oak Ridge National Laboratory, (June 1989).

4. J. O. Johnson, ed., "A User's Manual for MASH 1.0 - A Monte Carlo Adjoint Shielding Code System," ORNL/TM-11778, Oak Ridge National Laboratory, (March 1992).

5. T. A. Gabriel, et al., "CALOR: A Monte Carlo Program Package for the Design and Analysis of Calorimeter Systems," Oak Ridge National Laboratory, ORNL/TM-5619 (1977).

6. J. F. Briesmeister, Ed. MCNP-A General Purpose Monte Carlo Code for Neutron and Photon Transport, LASL Report LA-7396-M, Rev.2 (Sept. 1986).

7. P. Cloth, et al., "HERMES, A Monte Carlo Program System for Beam Material Interaction Studies," KFA Jülich, Report Jul-2203 (1988).

8. N. Odano, J. O. Johnson, and R. A. Lillie, "Preliminary Shielding Analysis and Design of the Remote Maintenance Cells for the Proposed National Spallation Neutron Source (NSNS)," in *Proc. Topical Meeting on Nuclear Applications of Accelerator Technology*, Albuquerque, NM, Nov. 16-20, 1997.

9. J. O. Johnson, ed., "A User's Manual for MASH 2.0 - A Monte Carlo Adjoint Shielding Code System," ORNL/TM-11778/R2, Oak Ridge National Laboratory, (To be published).

10. C. O. Slater, "The XTORID and ISPL3D codes for plotting TORT activities," ORNL Internal Memo, March 25, 1996.

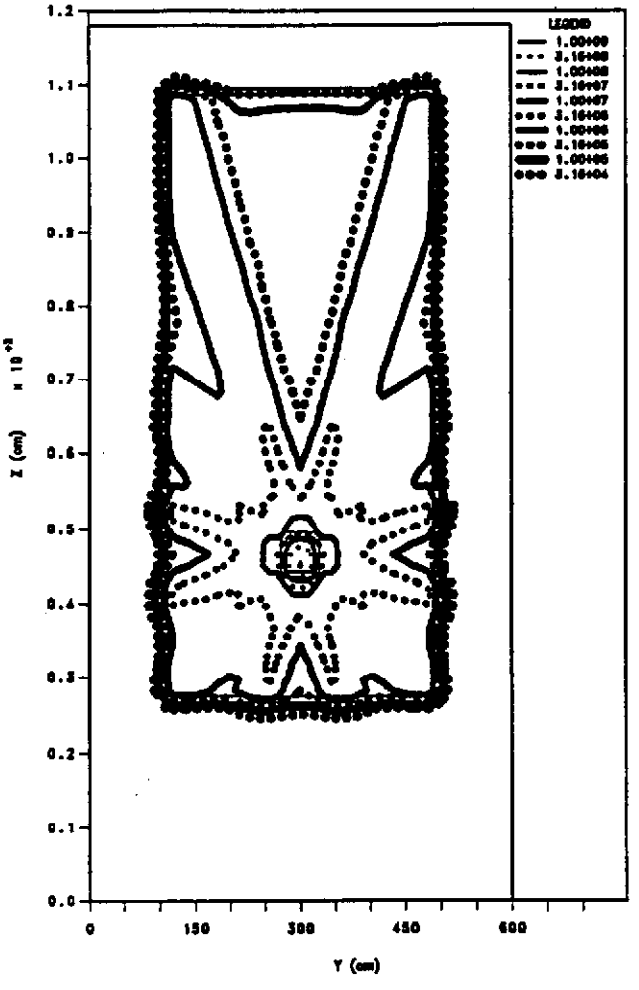

Fig. 3. Dose Contour Map (mrem/h) with TW Method Over y-z Plane in First Air Cell Inside the Left Wall

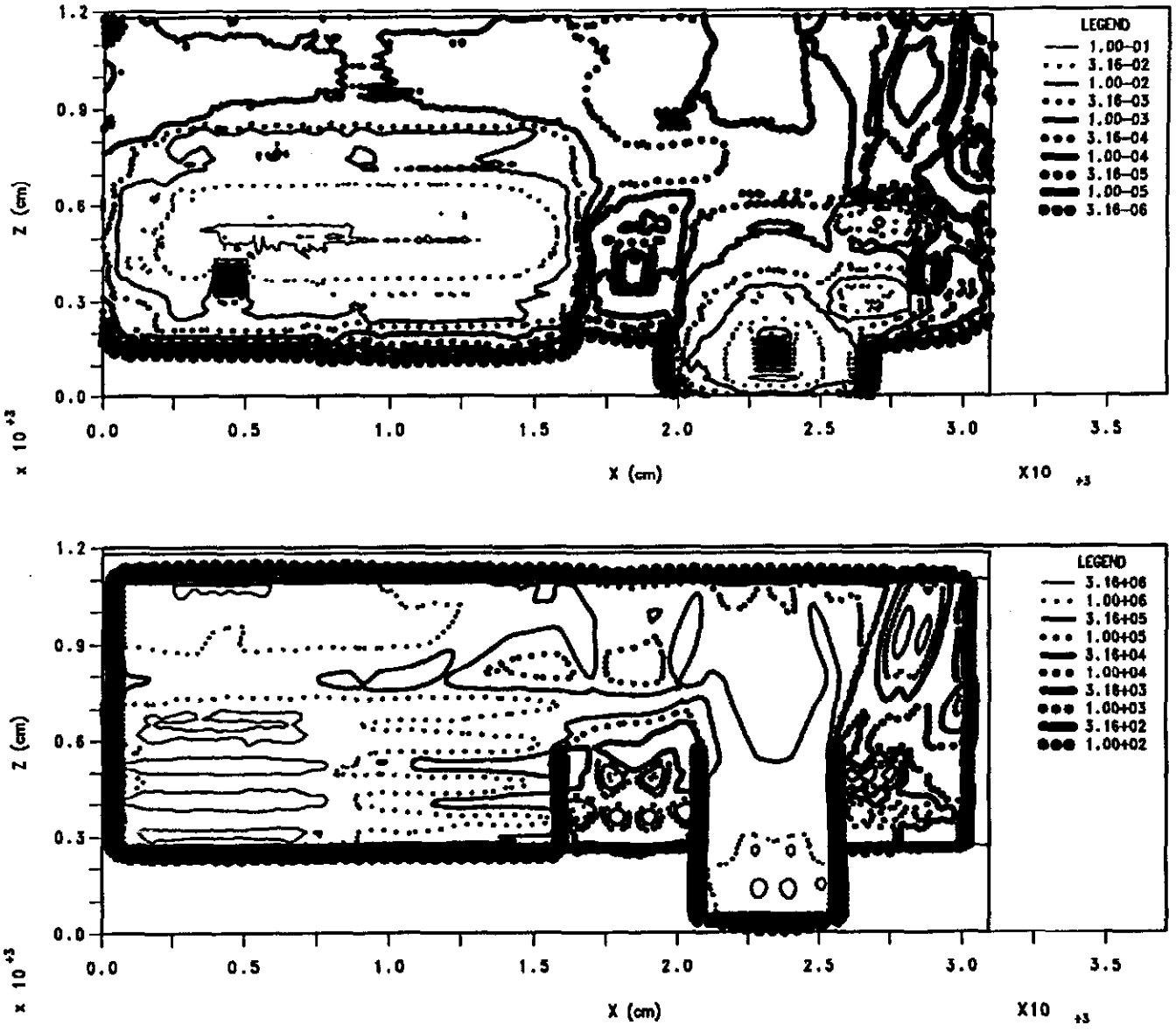

Fig. 4. Dose Contour Map (mrem/h) with TW Method Over x-z Plane in First Concrete (Top), and First Air Cell (Bottom) of the Near Wall

AZMY

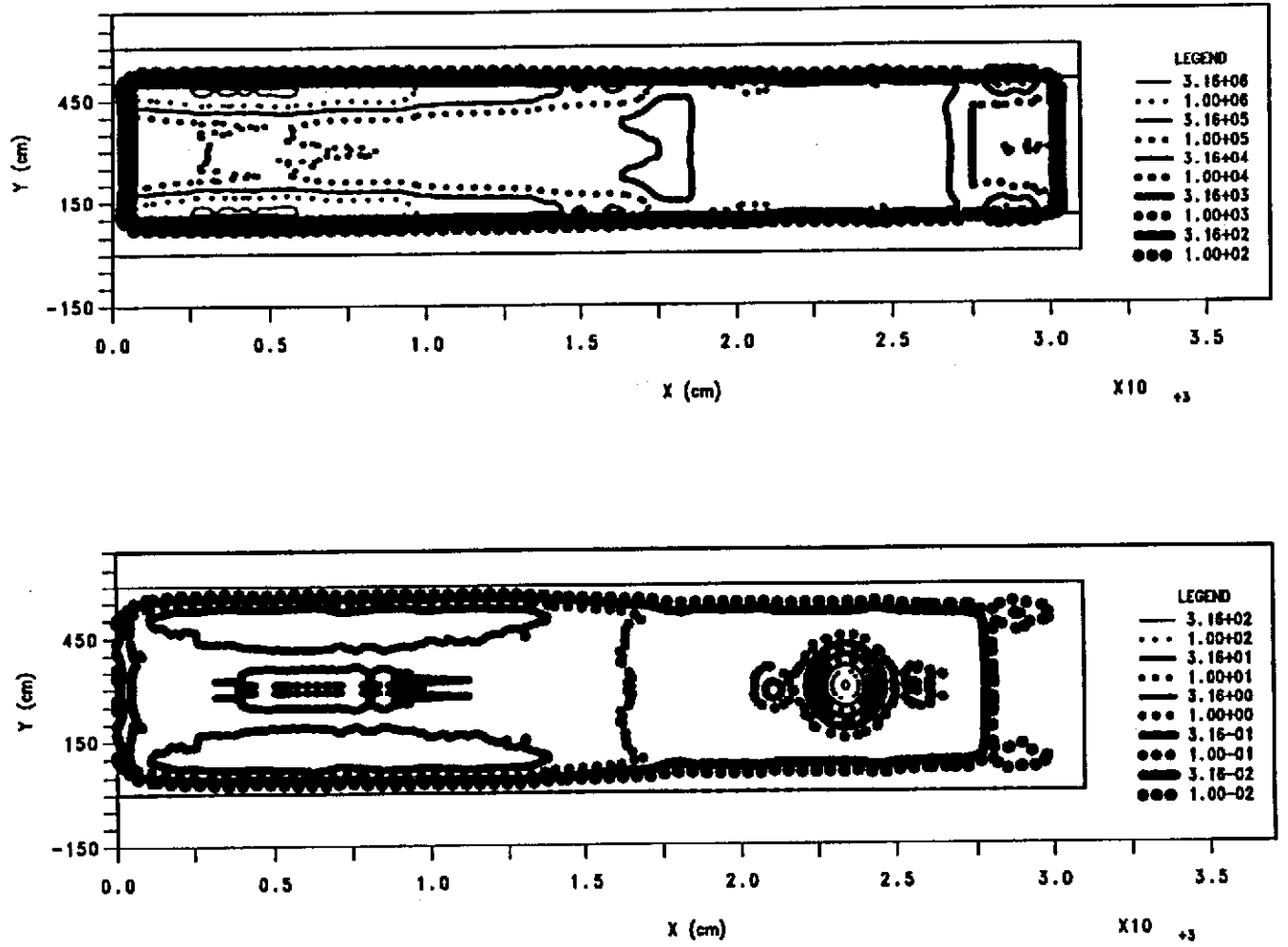

Fig. 5. Dose Contour Map (mrem/h) with TW Method Over x-y Plane in Last Air (Top), and Last Concrete Cell (Bottom) of the Ceiling

AZMY

10